



Anode potentials regulate *Geobacter* biofilms: New insights from the composition and spatial structure of extracellular polymeric substances

Guiqin Yang^a, Lingyan Huang^b, Zhen Yu^c, Xiaoming Liu^c, Shanshan Chen^b, Jianxiong Zeng^b, Shungui Zhou^b, Li Zhuang^{a,*}

^a Guangdong Key Laboratory of Environmental Pollution and Health, School of Environment, Jinan University, Guangzhou, 510632, China

^b Fujian Provincial Key Laboratory of Soil Environmental Health and Regulation, College of Resources and Environment, Fujian Agriculture and Forestry University, Fuzhou, 350002, China

^c Guangdong Key Laboratory of Integrated Agro-environmental Pollution Control and Management, Guangdong Institute of Eco-environmental Science & Technology, Guangzhou, 510650, China

ARTICLE INFO

Article history:

Received 10 September 2018

Received in revised form

20 April 2019

Accepted 8 May 2019

Available online 9 May 2019

Keywords:

Bioelectrochemical system

Geobacter soli

Anode potentials

Extracellular polymeric substances

Extracellular electron transfer

ABSTRACT

The extracellular electron transfer (EET) efficiency in bioelectrochemical systems has been proven to be dependent on anode potentials. To explore the underlying mechanism, previous studies have mainly focused on EET conduit and bacterial biomass but rarely concerned with the role of extracellular polymeric substances (EPS) surrounding electroactive cells. In this study, the response of *Geobacter* biofilms to anode potentials was investigated with a special emphasis on the mechanistic role of EPS. The electrochemical activities and cell viabilities of *Geobacter soli* biofilms were simultaneously attenuated at 0.4 and 0.6 V compared to −0.2 and 0 V. It was found that the biofilms (especially the biofilm region closer to electrode surface) grown at −0.2 and 0 V produced relatively more extracellular redox-active proteins and less extracellular polysaccharides, which conferred higher electron accepting/donating capacities to EPS and consequently facilitated EET. Meanwhile, electrically nonconductive extracellular polysaccharide-dominated interior layers were formed in the biofilms grown at 0.4 and 0.6 V, which limited direct EET but might serve as physical barriers for protecting cells in these biofilms from the increasing stress by poised electrodes. These results demonstrated that the production of EPS under different anode potentials might be finely regulated by cells to keep balance between EET efficiency and cell-protection. This study provides a new insight to investigate the *Geobacter* biofilms coping with various environments, and is useful for optimizing electrochemical activity of anode biofilms.

© 2019 Elsevier Ltd. All rights reserved.

1. Introduction

Bioelectrochemical systems (BESs) are engineered systems in which electroactive bacteria are grown under electrochemical interactions with electrodes (Hirose et al., 2018). These systems have attracted wide attention owing to their utility in various biotechnological processes, including electrical current generation from organic wastewater, production of useful chemicals, and environmental remediation (Sevda et al., 2018). In a BES, the anode functions as a terminal electron acceptor for microbial metabolism. A growing number of studies have shown that anode potentials

primarily determine the rate of electron flow from electroactive bacteria to electrodes and control the theoretical metabolic energy gained for microbial growth (Hirose et al., 2018).

Geobacter and *Shewanella* species are the most attractive electroactive bacteria in BESs (Kumar et al., 2017). For facultative anaerobic *Shewanella*, biofilms grown at high anode potentials are superior in current generation than that at middle or low potentials (Kitayama et al., 2017; Hirose et al., 2018); however, for anaerobic *Geobacter* or community predominated by *Geobacter*, current generation is commonly improved at relatively negative potentials (Wagner et al., 2010; Li et al., 2017; Zhu et al., 2014). In theory, more positive potentials are thermodynamically favorable for energy capture for bacterial growth (Wei et al., 2010), and therefore, it is inexplicable that why *Geobacter* biofilms produced lower current at

* Corresponding author.

E-mail address: zhuangli@jnu.edu.cn (L. Zhuang).

more positive potentials. For extracellular electron transfer (EET) through *Geobacter* biofilms, a pili network (nanowires) and redox-active proteins associated with the outer-membranes and localized in the extracellular matrix are essential (Kumar et al., 2017). Several previous studies based on voltammetry have proposed that *Geobacter* can alter the interfacial redox-active proteins at different anode potentials (Zhu et al., 2012; Peng et al., 2016). There is also voltammetric evidence indicating that the interfacial redox proteins in *Geobacter* biofilms are not affected by anode potentials (Wei et al., 2010), and the limited current generation at more positive potentials is due to the decreased cell viability by unknown reason (Li et al., 2017). Overall, no clear and plausible mechanisms have been proposed to explain how anode potentials regulate the EET properties of *Geobacter* biofilms.

As the major constituents of biofilms, extracellular polymeric substances (EPS) are generally considered as networks of organic material, including polysaccharides, proteins and lipids (Xue et al., 2012), and play multiple roles in promoting the structural development of biofilm and providing a protective barrier against environmental stress (Jia et al., 2017; Sheng et al., 2010). In addition to promoting biofilm formation, EPS produced by *Geobacter* cells also contributed to the electrochemical activities of the biofilms due to the redox-active proteins trapped therein (Rollefson et al., 2011; Magnuson, 2011). To date, studies associated with EPS in *Geobacter* biofilms have primarily focused on redox protein and exopolysaccharide content using gel electrophoresis and microscopy (Rollefson et al., 2011; Magnuson, 2011; Cologgi et al., 2014), while the composition and spatial distribution of EPS in *Geobacter* biofilms have not yet been adequately elucidated. As EPS production is easily affected by operational conditions (Jia et al., 2017), it is expected that the properties of EPS will vary depending on anode potentials. Considering the important contributions of EPS to EET in *Geobacter* biofilms (Liu et al., 2018), the effect of such EPS variations on electrochemical characteristics of *Geobacter* biofilms is worth studying.

Therefore, in the present study, BESs with *Geobacter soli* as inoculum were constructed and operated at six different anode potentials 1) to examine how EPS in *Geobacter* biofilms vary based on the change of anode potentials and 2) to elucidate the relationship between EPS composition and the electrochemical activities and structures of *Geobacter* biofilms. To the best of our knowledge, this is the first study to investigate the regulation of electroactive biofilms in the context of EPS. *Geobacter soli* was used here because of its great efficiency for EET, high similarity to other important *Geobacter* species such as *Geobacter sulfurreducens* and *Geobacter anodireducens* based on 16S rRNA gene sequences, and the available genetic information (Yang et al., 2015, 2017; Cai et al., 2018).

2. Materials and methods

2.1. Bacterial strain and reactor operation

Geobacter soli GSS01 was isolated and identified in our laboratory (Zhou et al., 2014), and was routinely cultured in freshwater medium at 30 °C under anaerobic conditions with acetate (16 mM) as the electron donor and Fe(III) citrate (56 mM) as the electron acceptor (Nevin et al., 2009).

Dual-chamber BES (triplicates for each treatment) with a volume of 250 mL for each chamber was constructed. Graphite plates were used as the working and counter electrodes, and a saturated calomel electrode (SCE) was used as the reference electrode. The working electrodes were separately controlled at -0.4 V, -0.2 V, 0 V, 0.2 V, 0.4 V and 0.6 V vs. SCE in individual reactor using a CHI1000C electrochemical station (CH Instruments Inc, Shanghai,

China). Current measurement was collected for at least 12 h prior to inoculation, and then, log-phase cultures of *G. soli* were inoculated (10%, v/v) into the working chamber containing freshwater medium with both acetate (10 mM) and Fe(III) citrate (56 mM). Once the cells reached A_{600} of ca. 0.2, the medium was replaced with freshwater medium containing acetate only. When the current reached approximately 1 mA, the system was switched to a continuous flow-through mode at a dilution rate of 0.15/h. The system was operated continuously for approximately 24 h after a constant current was reached, and then the biofilms were electrochemically characterized by differential pulse voltammetry (DPV) as documented in the literature (Pous et al., 2016).

2.2. Biomass, cell viability and cellular stress evaluation in biofilm

The biomass of biofilms was measured by Bacterial Protein Extraction Kit and BCA Protein Assay Kit (Sangon Biotech, China). Viability of the cells in biofilms was detected using confocal laser scanning microscopy (CLSM) (Sun et al., 2015; Xiao et al., 2017). The anodes were rinsed in sterile PBS to eliminate the growth medium, stained for 20 min using a LIVE/DEAD BacLight Bacterial Viability Kit (Invitrogen, CA), rinsed in sterile PBS twice to eliminate excess dye, and examined by CLSM (LSM 880, Carl Zeiss). The three-dimensional (3D) biofilm structure (z-stack) was reconstructed and analyzed using ZEN 2011 (Blue Edition, Carl Zeiss). The specific viability of each biofilm layer was analyzed and presented by the ratio of viable/total cells via software Image-Pro Plus 6.0 (Xiang et al., 2017).

The cellular stress was evaluated by two universal stress response proteins catalase (CAT) and superoxide dismutase (SOD), as their expression has been reported to be increased under environmental stress such as heavy metal toxicity and nutrient limitation (Holmes et al., 2006; Mouser et al., 2009; Orellana et al., 2014; Marozava et al., 2014). Kit S0051 and Kit S0101 (Beyotime Biotechnology, China) were used for determining the activities of CAT and SOD, respectively. The specific enzymes activities were presented as units per mg of total protein.

2.3. Spatial structure, composition and redox activity of EPS

2.3.1. The spatial structure of EPS

The anode biofilms were rinsed in PBS to eliminate growth medium and stained with FITC, ConA, calcofluor white and Nile red for the detection of proteins, α -polysaccharides, β -polysaccharides and lipids, respectively, in the EPS (Chen et al., 2007). Briefly, 0.1 M sodium bicarbonate buffer (pH 9.0, 200 μ l) was added to the electrode to maintain the amine group in a non-protonated form, followed by incubation with FITC solution (1 g/L, 100 μ l) for 1 h. Subsequently, the electrode was incubated with ConA solution (250 mg/L, 200 μ l) for another 30 min, followed successively by calcofluor white (300 mg/L, 200 μ l) for 30 min, and Nile red (10 mg/L, 120 μ l) for 10 min. After each stage of staining, the samples were washed twice with PBS to remove the excess stain. Then, the electrode was examined with a CLSM (LSM 880, Carl Zeiss) with a 40 \times objective. The collection wavelengths of all stains are listed in Table S1. The 3D biofilm structure was reconstructed and analyzed using ZEN 2011 (Blue Edition, Carl Zeiss). The specific EPS composition of each biofilm layer was analyzed based on counting per area (obj./total) via software Image-Pro Plus 6.0 and presented by the ratio of specific/total EPS components.

2.3.2. EPS extraction and composition analysis

The biofilm on the electrode was peeled and the dispersed biomass was harvested. EDTA treatment for extraction and preparation of both loose-bound EPS (LB-EPS) and tight-bound EPS (TB-

EPS) fractions were carried out by following a previously reported protocol (Cao et al., 2011). The polysaccharide and protein concentrations were measured using the anthrone method (Loewus, 1952) and BCA protein Assay Kit (Thermo Scientific Pierce), respectively. The EPS were then analyzed using EEM-PARAFAC (Excitation-emission matrix and parallel factor analysis) to quantitatively determine the fluorescence components of EPS (Ye et al., 2018).

2.3.3. Redox ability of EPS

As an index of redox capability, the electron accepting capacity (EAC) and electron donating capacity (EDC) were determined through electrochemical approaches as previously reported (Aeschbacher et al., 2010; Chen et al., 2017; Ye et al., 2018). To quantify the EAC and EDC of EPS, chronoamperometry measurements were performed at an applied potential of -0.73 V and $+0.37$ V (vs. SCE), respectively, and the transferred amount of electrons (TAE) was obtained by integration of the reductive or oxidative currents over time. The data of LB-EPS and TB-EPS were counted up to study the EDC and EAC of the total EPS of each biofilm. The expression of redox-active protein was assessed using reverse transcription quantitative real-time PCR (RT-qPCR). The target genes (namely SE37_01745, SE37_02820 and SE37_04285) were selected based on the genome and transcriptome analysis of *G. soli* (Yang et al., 2015; Cai et al., 2018). Annotations of the target genes and primers used for RT-qPCR are listed in Table S2. Gene expression levels were normalized to the expression level of *proC*, a gene shown to be constitutively expressed in *Geobacter* species (Holmes et al., 2005).

3. Results and discussion

3.1. Enhanced electrochemical activity of biofilms at -0.2 and 0 V

The time course of current production and the maximum current generated by *G. soli* grown at various anode potentials were compared (Fig. 1A and B). The biofilm grown at -0.4 V had the lowest maximum current (3.8 mA), which might be due to the limitation of electron acceptor, as this potential is close to the oxidation potential of acetate (-0.52 V vs. SCE) and is thermodynamically unfavorable for energy capture (Peng et al., 2016). An enhancement in current generation was observed when the anode potentials increased from -0.4 to 0 V, with a maximum current of 9.2 mA observed at -0.2 and 0 V, which indicated that -0.2 V is positive enough for BES with *G. soli*. When the anode potentials were further increased to 0.6 V, the maximum current was then decreased to 6.2 mA. These results were consistent with previous reports that current generation by *Geobacter* biofilm is higher at relatively negative potentials (Wei et al., 2010; Li et al., 2017).

DPV was used to measure the electrochemical activities of *G. soli* biofilms at different potentials, as it can show redox peaks of effective electrode reductases under catalytic conditions (Peng et al., 2016; Pous et al., 2016). Biofilms grown at -0.4 V showed three redox peaks with mid-point potentials of about -0.518 V, -0.378 V and -0.241 V, biofilms at -0.2 – 0.2 V showed two redox peaks with mid-potentials of -0.486 – -0.499 V and -0.305 – -0.341 V (Fig. 1C and Table S3). However, no obvious peaks were detected in the biofilms grown at 0.4 and 0.6 V, suggesting that the contents of interfacial redox-active proteins interacting with the electrodes in these biofilms might be sharply

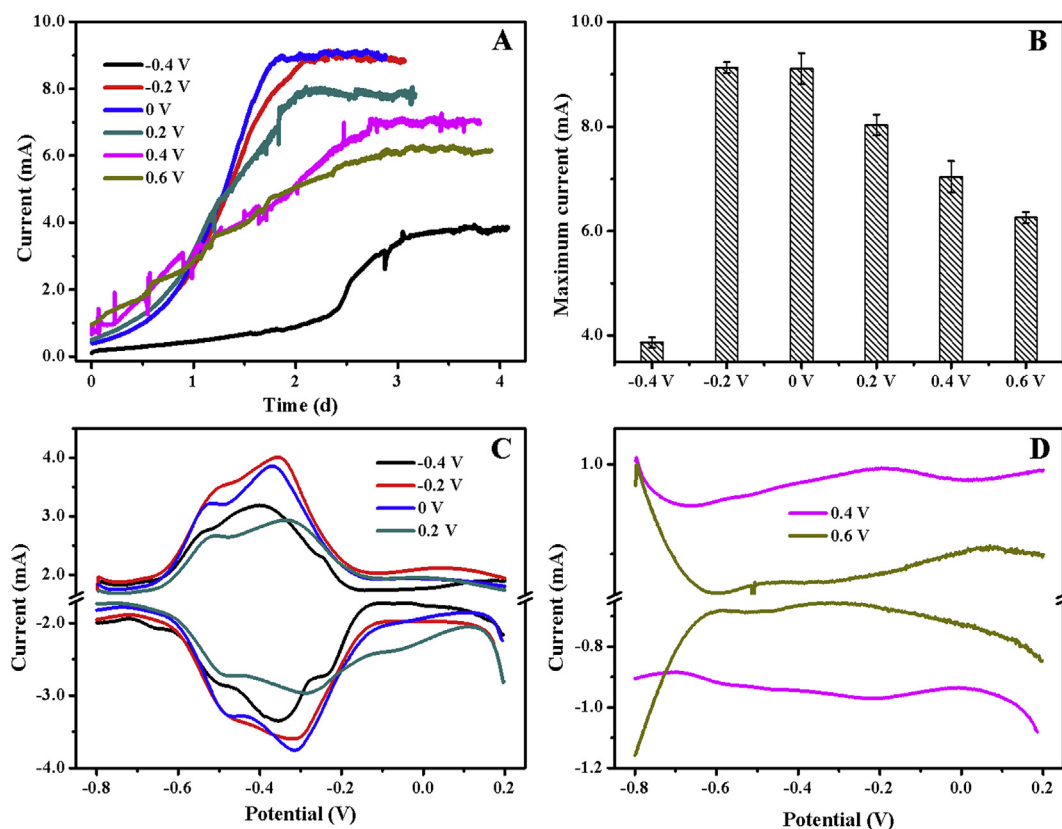


Fig. 1. Current production at various anode potentials (A), the maximum current produced at various anode potentials (B), and DPV analysis of biofilms cultured at anode potentials of -0.4 to 0.2 V (C), and at 0.4 and 0.6 V (D).

decreased for some reason (Fig. 1D). The difference in the number of redox pairs and their midpoint potentials supported the controversial hypothesis that interfacial redox-active proteins that directly interact with electrodes are affected by anode potentials (Zhu et al., 2012; Peng et al., 2016). Except for biofilm grown at -0.4 V, the peak currents of oxidation and reduction peaks of biofilms grown in the potential range of -0.2 – 0.6 V were strongly positively related to the maximum currents generated ($R^2 = 0.981$ and 0.968 for oxidation and reduction peak, respectively; $P < 0.05$) (Fig. S1), suggesting that the current generation of biofilms grown at potentials ranging from -0.2 – 0.6 V lied on the effective redox-active proteins interacting with the electrodes.

3.2. Decreased viability and increased biofilm heterogeneity at 0.4 and 0.6 V

The -0.4 V electrode was covered by a thinnest biofilm (~ 15 μm) (Fig. 2A) and the lowest biomass (Fig. 2B), which might be responsible for the lowest current generation at this potential. Weak cell adhesion to the electrode might be attributed to a low biomass gained at this potential, since *Geobacter* cells are negatively charged and the electrode poised at -0.4 V should encounter more difficulties in attracting negatively charged bacteria (Kuzume et al., 2013; Maestro et al., 2014). An increase in biofilm thickness and biomass was observed when the potentials increased from -0.2 to 0.2 V, and no increase was observed when the

potential further increased from 0.2 to 0.6 V (Fig. 2 and S2). It is logical that the biomass accumulation was enhanced in the potential range of 0.2 – 0.6 V compared with -0.4 – 0 V, as more positive potentials are favorable for cell adhesion and energy capture for microbial growth thermodynamically (Wei et al., 2010; Zhu et al., 2012). A similar average cell viability of approximately 0.74 was observed for biofilms grown at -0.2 and 0 V, and decreased viability of biofilms was observed with potentials increased from 0.2 to 0.6 V, ranging from 0.68 ± 0.07 for biofilm grown at 0.2 V to 0.42 ± 0.11 for biofilm grown at 0.6 V (Fig. 2B). As viable cells are responsible for electron production, the decreased cell viability might be a reason for the declined electrical current generation by biofilms.

Heterogeneous distribution of viable cells within all biofilms was observed, that is, the outer biofilm layer consisted of more viable cells and the inner layer consisted of more dead cells (Fig. 2A and S2). The two-layer structure of *Geobacter* biofilm has been previously reported, which is proposed as a result of transfer resistance of electron donors and gradient of protons accumulated within biofilm (Franks et al., 2009; Renslow et al., 2013). It is noticed that the viability in biofilms grown at 0.4 and 0.6 V, especially at 0.6 V, was more heterogeneous. In comparison, the maximum viability (0.91 ± 0.1) was 1.8 times of the minimum viability (0.50 ± 0.06) in biofilm grown at 0 V, whereas the maximum viability (0.62 ± 0.14) was 3.1 times of the minimum viability (0.20 ± 0.07) in biofilm grown at 0.6 V. In addition, even in

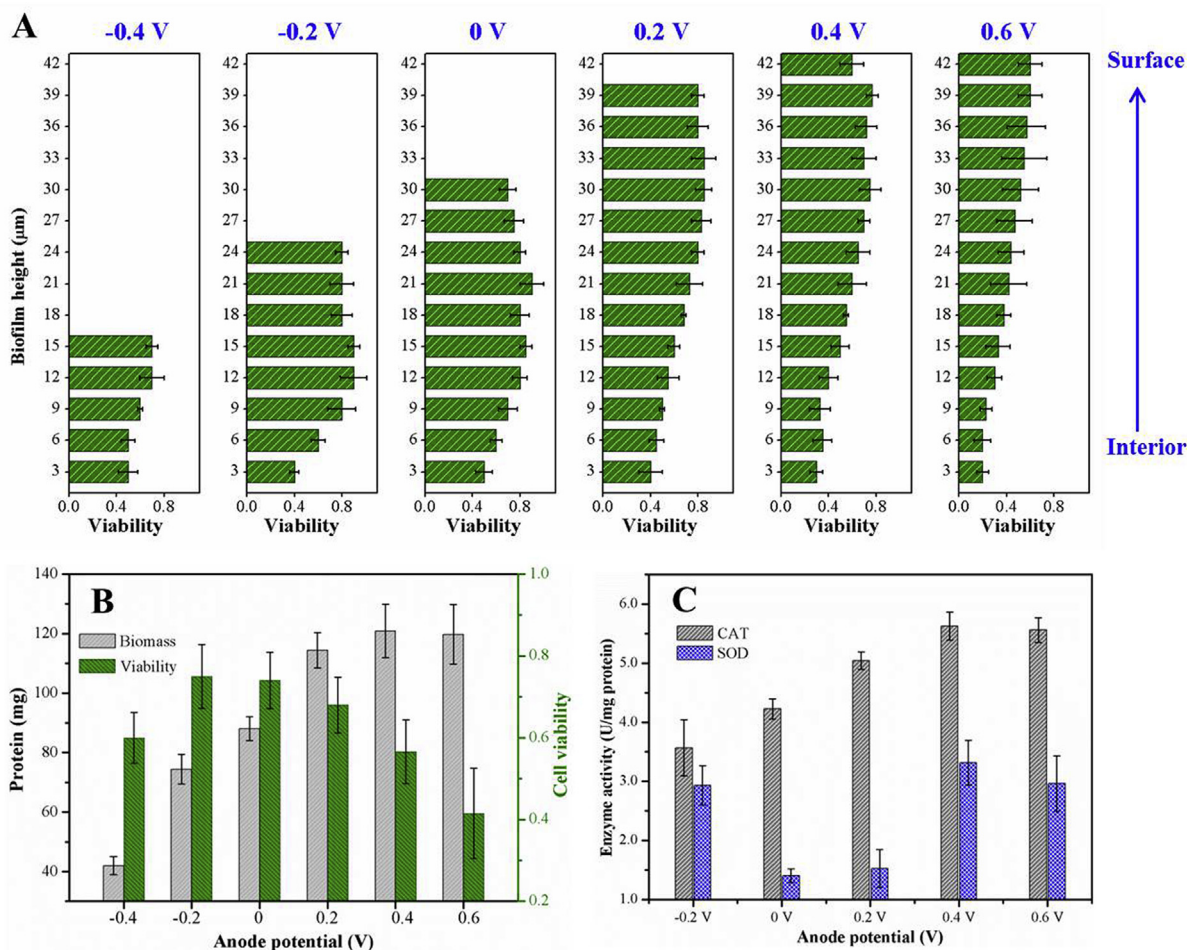


Fig. 2. Viability profiles (A), biomass and average viability (B), and enzyme activities of catalase (CAT) and superoxide dismutase (SOD) (C) of biofilms grown at different anode potentials.

the outer biofilm layers, the distribution of viable cells in biofilm grown at 0.6 V was also heterogeneous, presented as aggregated viable cells surrounded by inactive cells (Figs. S2F–H).

Cell aggregation is a protective strategy for microbes to resist environmental stress (Tsimring et al., 1995; Flemming et al., 2016). The activities of stress response proteins (SOD and CAT) in *G. soli* cells increased when the anode potentials rose from 0 to 0.6 V (Fig. 2C), showing that *G. soli* cells grown at 0.6 V were exposed to high stress induced by anode. It is likely that the increased stress is a potential cause of the decreased viability and increased heterogeneity of biofilms at 0.4 and 0.6 V, similar to a speculation in previous studies (Dennis et al., 2016).

3.3. Electrochemical activity of biofilm is positively related with redox activity of EPS

Considering the spatial distances, electrons generated by active cells cannot be directly transferred to electrodes when a thick layer of EPS covers the cell surface (Xiao et al., 2017). Fortunately, EPS have been proved to store electrochemically active substances, such as *c*-Cyts, which enable EPS-enveloped cells to transport extracellular electrons to acceptors (Cao et al., 2011; Rollefson et al., 2011; Zhang et al., 2016). Therefore, it is also important to evaluate EPS redox abilities of the biofilms grown at various electrode potentials.

As shown in Fig. 3A, the EPS of biofilm grown at 0 V had the maximum EDC (10.7 $\mu\text{mol e}^-/\text{g dry cell}$) and EAC (31.4 $\mu\text{mol e}^-/\text{g dry cell}$), followed by the EPS of biofilm grown at -0.2 V (9.6 and 30.0 $\mu\text{mol e}^-/\text{g dry cell}$ for EDC and EAC, respectively), and the weakest redox abilities were detected in the EPS of biofilms grown

at 0.4 and 0.6 V (4.2–4.3 $\mu\text{mol e}^-/\text{g dry cell}$ for EDC and 13.6–15.8 $\mu\text{mol e}^-/\text{g dry cell}$ for EAC). A positive correlation was found between EAC and peak current of reduction peak in DPV of biofilms ($R^2 = 0.867$; $P < 0.05$) and between EDC and peak current of oxidation peak ($R^2 = 0.673$; $P < 0.05$) (Fig. 3B and C). The EDC and EAC can reflect the redox activity of EPS (Ye et al., 2018) and the DPV reflects the electrochemical activity of biofilms (Pous et al., 2016), and therefore, this result indicated that the electrochemical activity of biofilm is positively related with redox activity of EPS.

EPS in biofilm functions as a conductive matrix for electron transfer to electrode, which is most likely mediated by outer-membrane and extracellular redox proteins (Liu et al., 2018; Xiao et al., 2017). The highest expression of three key genes encoding outer-membrane or extracellular *c*-Cyts in *G. soli* was observed in biofilm grown at 0 V, which was in agreement with the strongest redox ability of EPS (Fig. 3D).

3.4. *Geobacter soli* responds to anode potentials by regulating the EPS composition and spatial structure

Analysis of the EEM spectra using PARAFAC identified two aromatic protein-like substances with characteristic peaks at Ex/Em of 225/(335, 495) nm and (235, 280)/340 nm, which corresponded to tyrosine aromatic protein-like substance and tryptophan protein-like substance fluorophores, respectively (Fig. 4A and S3) (Jia et al., 2017; He et al., 2014). With the potentials increased from -0.4 – 0.6 V, the amount of tyrosine aromatic protein-like substances initially increased and then decreased in LB-EPS, whereas the amount of tryptophan protein-like substances first

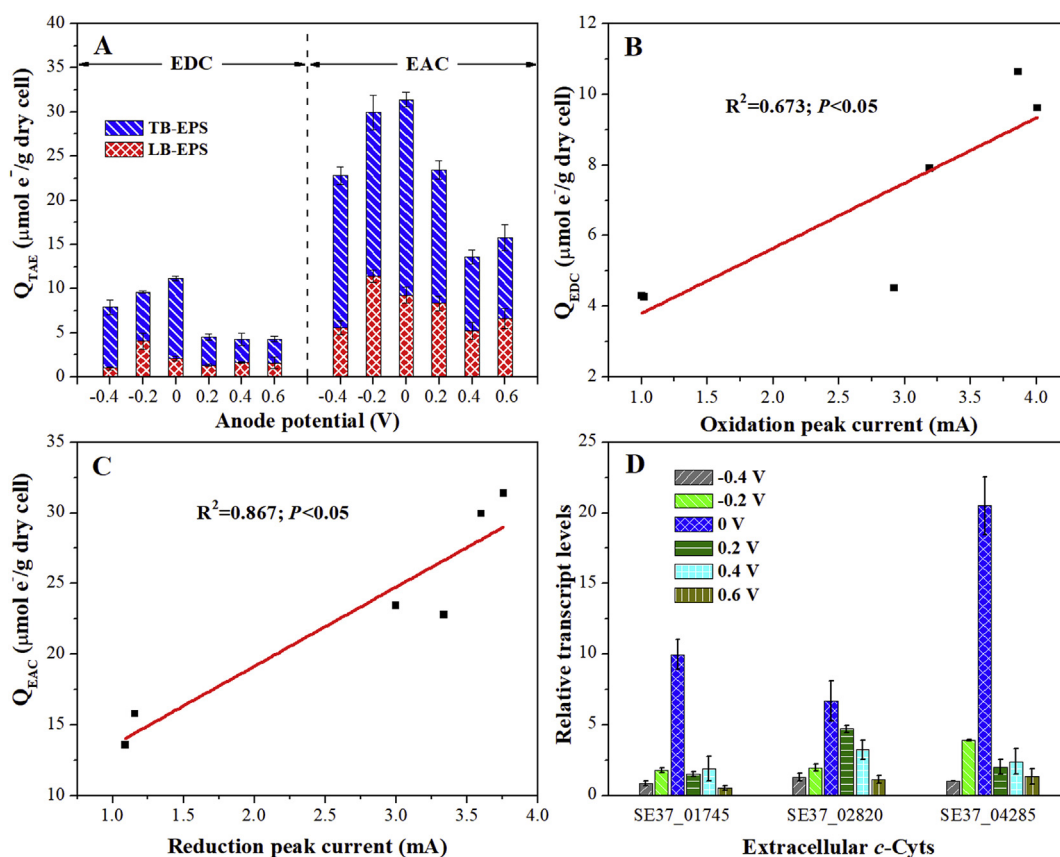


Fig. 3. Comparison of electron accepting capacity and electron donating capacity of total EPS extracted from biofilms grown at various anode potentials (A), electrochemical activity of various biofilms determined by electron transferring capacity of EPS (B and C), and the transcript levels of three key genes encoding outer-membrane or extracellular *c*-Cyt in *G. soli* cells cultured at various anode potentials (D).

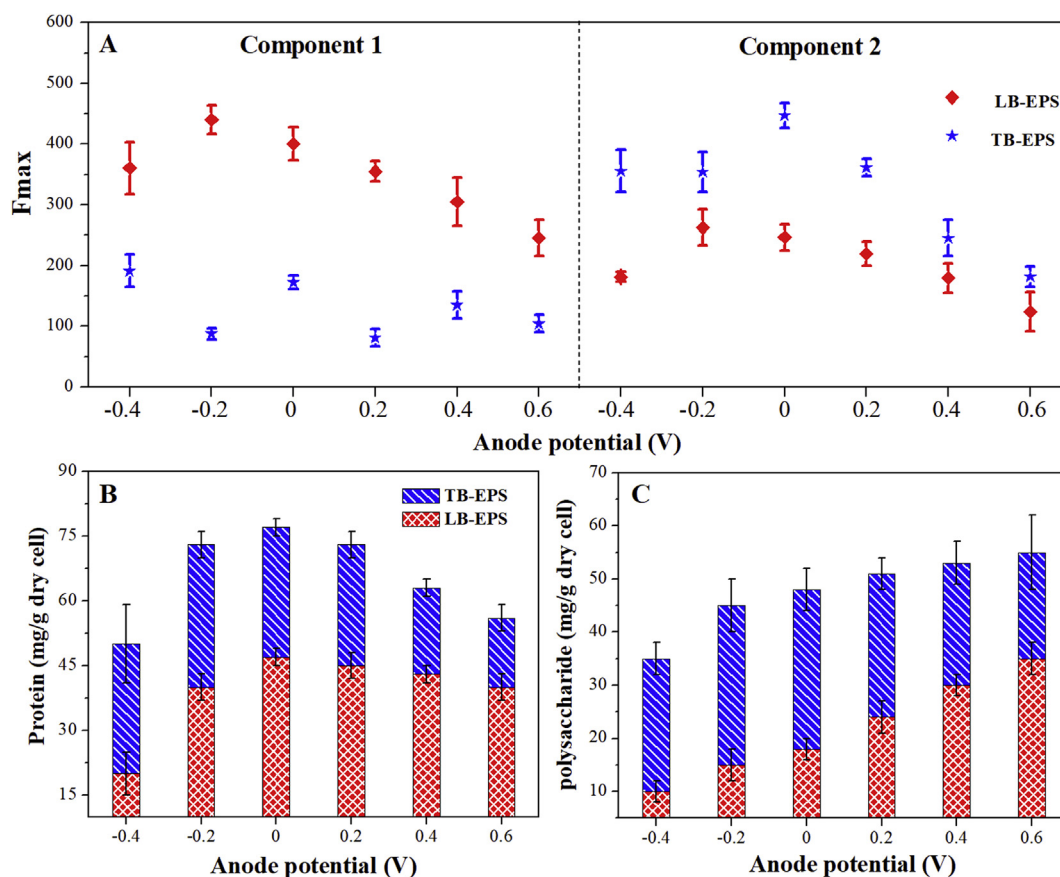


Fig. 4. The effect of anode potentials on two fluorescence components analyzed by the EEM-PARAFAC model: tyrosine aromatic protein-like substance (Component 1) and tryptophan protein-like substance (Component 2) (A), and the effect of anode potentials on the composition of EPS, polysaccharide (B) and protein (C) determined by chemical detection.

increased and then decreased in both LB-EPS and TB-EPS. The aromatic amino acids play an important role in electron transfer (Hirasawa et al., 1998; Görner, 2007; Vargas et al., 2013), and thus the reduction of the two aromatic protein-like substances in EPS might be responsible for the decreased redox activity of EPS of biofilms grown at 0.4–0.6 V.

With the potentials increased from –0.2–0.6 V, the concentration of extracellular polysaccharide was increased while the production of extracellular protein was reduced (Fig. 4B and C). In addition, the EPS components in all biofilms were found to be heterogeneously distributed throughout the entire biofilm (Fig. 5). Compared to the interior layer of biofilm grown at –0.2 V, which contained higher proportion of proteins (42.4%), the interior layers of biofilms grown at 0.4 and 0.6 V were predominated by extracellular polysaccharides (41.1–60.7%) (Fig. S5). These results suggested that *G. soli* cells, especially the cells in the interior layer of the biofilm, stimulated the production of extracellular polysaccharide by higher potentials (0.4 and 0.6 V). The maximum current generated by biofilms grown in the potential range of –0.2–0.6 V was positively related to protein content but negatively related to extracellular polysaccharide content in EPS of the entire biofilm ($R^2 > 0.87$, $P < 0.05$) (Figs. S6A and C). This correlation was also applied to the interior biofilm layers ($R^2 > 0.86$; $P < 0.05$) (Figs. S6B and D) but not to the middle and outer biofilm layers (data not shown), which agreed with the result in section 3.1 that

current generation of biofilms grown at potentials ranging from –0.2–0.6 V lied on the effective redox-active proteins interacting with the electrodes.

According to a model of mechanistic stratification in electroactive biofilms, the EPS-associated redox-active proteins function coordinately with conductive pili to transfer electrons in the region (within 10 μm) closer to the electrode; however, the pili networks become as the primary mechanism for discharging electrons in the upper region (>10 μm) (Steidl et al., 2016). That is, electron transfer mediated by EPS-associated redox-active proteins mainly occurs in the region closer to the electrode, and therefore, the EPS composition in the interior biofilm layers might play an essential role in determining the EET efficiency of biofilms. As previously reported, electron transfer in electroactive biofilms is mainly taken charge by the outer membrane and extracellular redox-active proteins (Kumar et al., 2017) while nonconductive polysaccharides can interfere with EET between redox-active proteins and electrodes (Kouzuma et al., 2010; Kitayama et al., 2017). Thus, the predominant presence of extracellular polysaccharides (especially in the interior biofilm layers) might be a direct cause for the low electrochemical activity of biofilms grown at 0.4 and 0.6 V in the present study.

Extracellular polysaccharide production is often activated by environmental stress for cell-protection (Gambino and Cappitelli, 2016; Han et al., 2017); this might be a potential reason for the

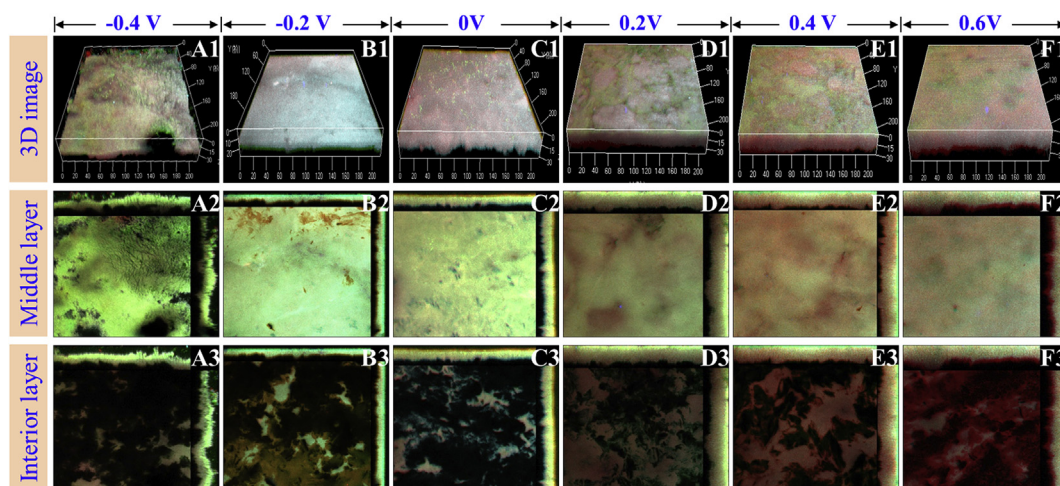


Fig. 5. Heterogeneous distribution of EPS components scattered in biofilms cultured at potentials of -0.4 (A), -0.2 (B), 0 (C), 0.2 (D), 0.4 (E) and 0.6 V (F). 1, 3D images of biofilms; 2, middle layers of the biofilms (approximately $10\ \mu\text{m}$ from the biofilm surface); 3, interior layers of the biofilms (close to the electrode). The single signal from FITC, Con-A, calcofluor white and Nile red is shown in Fig. S4. The graphs present here are merged images containing signals from these four stains. (For interpretation of the references to colour in this figure legend, the reader is referred to the Web version of this article.)

accumulation of interfacial polysaccharides in *Geobacter* biofilms at 0.4 and 0.6 V exposing to high stress induced by anode (section 3.2). *Geobacter* species are anaerobic bacteria which commonly grow via reduction of metal (oxyhydr)oxides with low predicted redox potentials ranging from $+0.11$ V vs. SCE (e.g. birnessite) to -0.41 V vs. SCE (e.g. $\alpha\text{-FeOOH}$) (Elevar et al., 2017). Therefore, high potentials of 0.4 and 0.6 V might induce stress response in *Geobacter* cells, and activate the production of extracellular polysaccharides for self-protection purpose. If cells exposing to excessive stress are not protected by EPS, proteins on the cell surface are easily inactivated, even resulting in cell death and EET lost (Xiao et al., 2017; Han et al., 2017). By contrast, for facultative anaerobe *Shewanella* species that have developed perfect strategies to adapt quite positive oxidation potentials (e.g. oxygen; 0.99 V vs. SCE), the production of polysaccharides will not be stimulated under high anode potentials (Kitayama et al., 2017). Overall, the production of EPS under different anode potentials would be finely regulated by cells to keep balance between EET efficiency and cell-protection. This might be an important underlying mechanism for tuning the electrochemical properties of biofilms at various anode potentials, which are helpful to better understand how to set and evaluate optimal anode potentials for improving BES performance.

4. Conclusion

In this work, *Geobacter soli* biofilms grown at -0.2 and 0 V were found to have higher electrochemical activity and EET efficiency than those grown at higher potentials ranging from 0.2 to 0.6 V, although more positive potential is thermodynamically favorable for microbial metabolism. It was demonstrated that biofilms grown at -0.2 and 0 V possessed higher cell viability, and thereby generated more electrons from cellular metabolism than those grown at 0.2 , 0.4 and 0.6 V. Meanwhile, higher concentrations of protein were detected in EPS of the biofilms grown at -0.2 and 0 V, resulting in higher redox activity of EPS and greater EET efficiency in these biofilms. The accumulation of electrically nonconductive extracellular polysaccharide in the biofilm grown at 0.4 and 0.6 V, especially in the region closer to electrodes, will dramatically interfere with electron transfer from redox-active proteins to electrodes but be favorable for cell protection. These findings provide a new insight for deep understanding the regulation of

electroactive biofilms for optimal performance, and can be useful for elucidating the mechanisms how biofilms respond to environmental changes.

Declarations of competing interest

The authors declare that the research was conducted in the absence of any commercial or financial relationships that could be construed as a potential conflict of interest.

Acknowledgements

Financial support was provided by the National Natural Science Foundation of China (41671264 and 91751109), and Guangdong Special Support Program (2017TX04Z351).

Appendix A. Supplementary data

Supplementary data to this article can be found online at <https://doi.org/10.1016/j.watres.2019.05.027>.

References

- Aeschbacher, M., Sander, M., Schwarzenbach, R.P., 2010. Novel electrochemical approach to assess the redox properties of humic substances. *Environ. Sci. Technol.* 44, 87–93.
- Cai, X., Huang, L., Yang, G., Yu, Z., Wen, J., Zhou, S., 2018. Transcriptomic, proteomic, and bioelectrochemical characterization of an exoelectrogen *Geobacter soli* grown with different electron acceptors. *Front. Microbiol.* 9, 1075.
- Cao, B., Shi, L., Brown, R.N., Xiong, Y., Fredrickson, J.K., Romine, M.F., Marshall, M.J., Lipton, M.S., Beyenal, H., 2011. Extracellular polymeric substances from *Shewanella* sp. HRCR-1 biofilms: characterization by infrared spectroscopy and proteomics. *Environ. Microbiol.* 13, 1018–1031.
- Chen, S., Jing, X., Tang, J., Fang, Y., Zhou, S., 2017. Quorum sensing signals enhance the electrochemical activity and energy recovery of mixed-culture electroactive biofilms. *Biosens. Bioelectron.* 97, 369–376.
- Chen, M., Lee, D., Tay, J., Show, K., 2007. Staining of extracellular polymeric substances and cells in bioaggregates. *Appl. Microbiol. Biotechnol.* 75, 467–474.
- Cologgi, D.L., Speers, A.M., Bullard, B.A., Kelly, S.D., Reguera, G., 2014. Enhanced uranium immobilization and reduction by *Geobacter sulfurreducens* biofilms. *Appl. Environ. Microbiol.* 80, 6638–6646.
- Dennis, P.G., Virdis, B., Vanwonterghem, I., Hassan, A., Hugenholtz, P., Tyson, G.W., Rabaey, K., 2016. Anode potential influences the structure and function of anodic electrode and electrolyte-associated microbiomes. *Sci. Rep.* 6, 39114.
- Elevar, C.E., Hoffman, C.L., Dunshee, A.J., Toner, B.M., Bond, D.R., 2017. Redox potentials as a master variable controlling pathways of metal reduction by *Geobacter sulfurreducens*. *ISME J.* 11, 741–752.

- Flemming, H., Wingender, J., Szewzyk, U., Steinberg, P., Rice, S.A., Kjelleberg, S., 2016. Biofilms: an emergent form of bacterial life. *Nat. Rev. Microbiol.* 14, 563–575.
- Franks, A.E., Nevin, K.P., Jia, H., Izallalen, M., Woodard, T.L., Lovley, D.R., 2009. Novel strategy for three-dimensional real-time imaging of microbial fuel cell communities: monitoring the inhibitory effects of proton accumulation within the anode biofilm. *Energy Environ. Sci.* 2, 113–119.
- Gambino, M., Cappitelli, F., 2016. Mini-review: biofilm responses to oxidative stress. *Biofouling* 32, 167–178.
- Görner, H., 2007. Electron transfer from aromatic amino acids to triplet quinones. *J. Photochem. Photobiol., B* 88, 83–89.
- Han, X., Wang, Z., Chen, M., Zhang, X., Tang, C.Y., Wu, Z., 2017. Acute responses of microorganisms from membrane bioreactors in the presence of NaOCl: protective mechanisms of extracellular polymeric substances. *Environ. Sci. Technol.* 51, 3233–3241.
- He, X., Xi, B., Cui, D., Liu, Y., Tan, W., Pan, H., Li, D., 2014. Influence of chemical and structural evolution of dissolved organic matter on electron transfer capacity during composting. *J. Hazard Mater.* 268, 256–263.
- Hirasawa, M., Hurley, J.K., Salamon, Z., Tollin, G., Markley, J.L., Cheng, H., Xia, B., Knaff, D.B., 1998. The role of aromatic and acidic amino acids in the electron transfer reaction catalyzed by spinach ferredoxin-dependent glutamate synthase. *BBA-Bioenergetics* 1363, 134–146.
- Hirose, A., Kasai, T., Aoki, M., Umemura, T., Watanabe, K., Kouzuma, A., 2018. Electrochemically active bacteria sense electrode potentials for regulating catabolic pathways. *Nat. Commun.* 9, 1083.
- Holmes, D.E., Chaudhuri, S.K., Nevin, K.P., Mehta, T., Methé, B.A., Liu, A., Ward, J.E., Woodard, T.L., Webster, J., Lovley, D.R., 2006. Microarray and genetic analysis of electron transfer to electrodes in *Geobacter sulfurreducens*. *Environ. Microbiol.* 8, 1805–1815.
- Holmes, D.E., Nevin, K.P., O'Neil, R.A., Ward, J.E., Adams, L.A., Woodard, T.L., Vrionis, H.A., Lovley, D.R., 2005. Potential for quantifying expression of the *Geobacteraceae* citrate synthase gene to assess the activity of *Geobacteraceae* in the subsurface and on current-harvesting electrodes. *Appl. Environ. Microbiol.* 71, 6870–6877.
- Jia, F., Yang, Q., Liu, X., Li, X., Li, B., Zhang, L., Peng, Y., 2017. Stratification of extracellular polymeric substances (EPS) for aggregated anammox microorganisms. *Environ. Sci. Technol.* 51, 3260–3268.
- Kitayama, M., Koga, R., Kasai, T., Kouzuma, A., Watanabe, K., 2017. Structures, compositions, and activities of live *Shewanella* biofilms formed on graphite electrodes in electrochemical flow cells. *Appl. Environ. Microbiol.* 83, e00903–e00917.
- Kouzuma, A., Meng, X.Y., Kimura, N., Hashimoto, K., Watanabe, K., 2010. Disruption of the putative cell surface polysaccharide biosynthesis gene SO3177 in *Shewanella oneidensis* MR-1 enhances adhesion to electrodes and current generation in microbial fuel cells. *Appl. Environ. Microbiol.* 76, 4151–4157.
- Kumar, A., Hsu, L.H., Kavanagh, P., Barrière, F., Lens, P.N.L., Lapinonnière, L., Lienhard V, J.H., Schröder, U., Jiang, X., Leech, D., 2017. The ins and outs of microorganism-electrode electron transfer reactions. *Nat. Rev. Chem.* 1, 0024.
- Kuzume, A., Zhumaev, U., Li, J., Fu, Y., Füg, M., Esteve-Núñez, A., Wandlowski, T., 2013. An in-situ surface electrochemistry approach toward whole-cell studies: charge transfer between *Geobacter sulfurreducens* and electrified metal/electrolyte interfaces through linker molecules. *Electrochim. Acta* 112, 933–942.
- Li, D., Huang, Y., Li, J., Li, L., Tian, L., Yu, H., 2017. Electrochemical activities of *Geobacter* biofilms growing on electrodes with various potentials. *Electrochim. Acta* 225, 452–457.
- Liu, X., Zhuo, S., Rensing, C., Zhou, S., 2018. Syntrophic growth with direct interspecies electron transfer between pilifree *Geobacter* species. *ISME J.* 12, 2142–2151.
- Loewus, F.A., 1952. Improvement in anthone method for determination of carbohydrate. *Anal. Chem.* 24, 219–219.
- Maestro, B., Ortiz, J.M., Schrott, G., Busalmen, J.P., Climent, V., Feliu, J.M., 2014. Crystallographic orientation and electrode nature are key factors for electric current generation by *Geobacter sulfurreducens*. *Bioelectrochemistry* 98, 11–19.
- Magnuson, T.S., 2011. How the *xap* locus put electrical “zap” in *Geobacter sulfurreducens* biofilms. *J. Bacteriol.* 193, 1021–1022.
- Marozava, S., Röling, W.F.M., Seifert, J., Küffner, R., Bergen, M.V., Meckenstock, R.U., 2014. Physiology of *Geobacter metallireducens* under excess and limitation of electron donors. Part II. Mimicking environmental conditions during cultivation in retentostats. *Syst. Appl. Microbiol.* 37, 287–295.
- Mouser, P.J., Holmes, D.E., Perpetua, L.A., DiDonato, R., Postier, B., Liu, A., Lovley, D.R., 2009. Quantifying expression of *Geobacter* spp. oxidative stress genes in pure culture and during in situ uranium bioremediation. *ISME J.* 3, 454–465.
- Nevin, K.P., Kim, B., Glaven, R.H., Johnson, J.P., Woodard, T.L., Methé, B.A., DiDonato, R.J., Covalla, S.F., Franks, A.E., Liu, A., Lovley, D.R., 2009. Anode biofilm transcriptomics reveals outer surface components essential for high density current production in *Geobacter sulfurreducens* fuel cells. *PLoS One* 4, e5628.
- Orellana, R., Hixson, K.K., Murphy, S., Mester, T., Sharma, M.L., Lipton, M.S., Lovley, D.R., 2014. Proteome of *Geobacter sulfurreducens* in the presence of U(VI). *Microbiology* 160, 2607–2617.
- Peng, L., Zhang, X., Yin, J., Xu, S., Zhang, Y., Xie, D., Li, Z., 2016. *Geobacter sulfurreducens* adapts to low electrode potential for extracellular electron transfer. *Electrochim. Acta* 191, 743–749.
- Pous, N., Carmona-Martínez, A.S., Vilajeliu-Pons, A., Fiset, E., Bañeras, L., Trably, E., Balaguer, M.D., Colprim, J., Bernet, N., Puig, S., 2016. Bidirectional microbial electron transfer: switching an acetate oxidizing biofilm to nitrate reducing conditions. *Biosens. Bioelectron.* 75, 352–358.
- Renslow, R.S., Babauta, J.T., Dohnalkova, A.C., Boyanov, M.I., Kemner, K.M., Majors, P.D., Fredrickson, J.K., Beyenal, H., 2013. Metabolic spatial variability in electrode-respiring *Geobacter sulfurreducens* biofilms. *Energy Environ. Sci.* 6, 1827–1836.
- Rollefson, J.B., Stephen, C.S., Tien, M., Bond, D.R., 2011. Identification of an extracellular polysaccharide network essential for cytochrome anchoring and biofilm formation in *Geobacter sulfurreducens*. *J. Bacteriol.* 193, 1023–1033.
- Sevda, S., Sreekishnan, T.R., Pous, N., Puig, S., Pant, D., 2018. Bioelectroremediation of perchlorate and nitrate contaminated water: a review. *Bioresour. Technol.* 255, 331–339.
- Sheng, G.P., Yu, H.Q., Li, X.Y., 2010. Extracellular polymeric substances (EPS) of microbial aggregates in biological wastewater treatment systems: a review. *Biotechnol. Adv.* 28, 882–894.
- Steidl, R.J., Lampa-Pastirk, S., Reguera, G., 2016. Mechanistic stratification in electroactive biofilms of *Geobacter sulfurreducens* mediated by pilus nanowires. *Nat. Commun.* 7, 12217.
- Sun, D., Cheng, S., Wang, A., Li, F., Logan, B.E., Cen, K., 2015. Temporal-spatial changes in viabilities and electrochemical properties of anode biofilms. *Environ. Sci. Technol.* 49, 5227–5235.
- Tsimring, L., Levine, H., Aranson, I., Ben-Jacob, E., Cohen, I., Shochet, O., Reynolds, W.N., 1995. Aggregation patterns in stressed bacteria. *Phys. Rev. Lett.* 75, 1859–1862.
- Vargas, M., Malvankar, N.S., Tremblay, P., Leang, C., Smith, J.A., Patel, P., 2013. Aromatic amino acids required for pili conductivity and long-range extracellular electron transport in *Geobacter sulfurreducens*. *mBio* 4, e00105–e00113.
- Wagner, R.C., Call, D.F., Logan, B.E., 2010. Optimal set anode potentials vary in bioelectrochemical systems. *Environ. Sci. Technol.* 44, 6036–6041.
- Wei, J., Liang, P., Cao, X., Huang, X., 2010. A new insight into potential regulation on growth and power generation of *Geobacter sulfurreducens* in microbial fuel cells based on energy viewpoint. *Environ. Sci. Technol.* 44, 3187–3191.
- Xiang, Y., Liu, G., Zhang, R., Lu, Y., Luo, H., 2017. High-efficient acetate production from carbon dioxide using a bioanode microbial electrosynthesis system with bipolar membrane. *Bioresour. Technol.* 233, 227–235.
- Xiao, Y., Zhang, E., Zhang, J., Dai, Y., Yang, Z., Christensen, H.E.M., Ulstrup, J., Zhao, F., 2017. Extracellular polymeric substances are transient media for microbial extracellular electron transfer. *Sci. Adv.* 3, e1700623.
- Xue, Z., Sendamangalam, V.R., Gruden, C.L., Seo, Y., 2012. Multiple roles of extracellular polymeric substances on resistance of biofilm and detached clusters. *Environ. Sci. Technol.* 46, 13212–13219.
- Yang, G., Chen, S., Zhou, S., Liu, Y., 2015. Genome sequence of a dissimilatory Fe(III)-reducing bacterium *Geobacter soli* type strain GSS01. *Stand. Genomic. Sci.* 10, 118.
- Yang, G., Huang, L., You, L., Zhuang, L., Zhou, S., 2017. Electrochemical and spectroscopic insights into the mechanisms of bidirectional microbe-electrode electron transfer in *Geobacter soli* biofilms. *Electrochem. Commun.* 77, 93–97.
- Ye, J., Hu, A., Ren, G., Chen, M., Tang, J., Zhang, P., Zhou, S., He, Z., 2018. Enhancing sludge methanogenesis with improved redox activity of extracellular polymeric substances by hematite in red mud. *Water Res.* 134, 54–62.
- Zhang, X., Yang, C., Yu, H., Sheng, G., 2016. Light-induced reduction of silver ions to silver nanoparticles in aquatic environments by microbial extracellular polymeric substances (EPS). *Water Res.* 106, 242–248.
- Zhou, S., Yang, G., Lu, Q., Wu, M., 2014. *Geobacter soli* sp. nov., a dissimilatory Fe(III)-reducing bacterium isolated from forest soil. *Int. J. Syst. Evol. Microbiol.* 64, 3786–3791.
- Zhu, X., Yates, M.D., Hatzell, M.C., Rao, H.A., Saikaly, P.E., Logan, B.E., 2014. Microbial community composition is unaffected by anode potential. *Environ. Sci. Technol.* 48, 1352–1358.
- Zhu, X., Yates, M.D., Logan, B.E., 2012. Set potential regulation reveals additional oxidation peaks of *Geobacter sulfurreducens* anodic biofilms. *Electrochem. Commun.* 22, 116–119.